

pg2013

by Muhamad Yusa

Submission date: 03-Apr-2021 09:30AM (UTC+0700)

Submission ID: 1549380076

File name: PG2013.pdf (536.6K)

Word count: 2338

Character count: 12503

4

Quantification of time-dependent microstructural change of a silty sand under load

2

Cite as: AIP Conference Proceedings 1542, 293 (2013); <https://doi.org/10.1063/1.4811925>

Published Online: 18 June 2013

M. Yusa, and E. T. Bowman



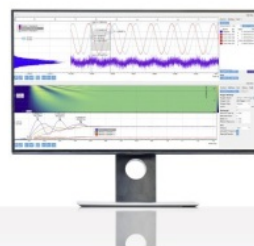
View Online



Export Citation

Challenge us.

What are your needs for
periodic signal detection?



Zurich
Instruments

2

AIP Conference Proceedings 1542, 293 (2013); <https://doi.org/10.1063/1.4811925>

1542, 293

© 2013 AIP Publishing LLC.

3

Quantification of Time-dependent Microstructural Change of a Silty Sand under Load

M. Yusa, and E.T. Bowman,

5

University of Canterbury Department of Civil and Natural Resources Engineering
Private Bag 4800, Christchurch New Zealand

1

Abstract. Imaging technology may be used in geotechnical engineering to enhance our understanding of microscopic characteristics and micro-mechanical behaviour of sands. In this study, silty sand samples loaded uniaxially under K_0 condition for ageing times of one hour and one week were preserved using low viscosity epoxy resin. High quality images were captured by scanning electron microscope utilizing a backscattered electron detector to give excellent contrast between the grains and the voids. Change in microstructure due to ageing is investigated statistically using particle orientation and distribution of spatial distance between particles in horizontal and vertical directions. It was found that although mean distance between particles only slightly reduces, overall ageing causes larger sand particles to rotate. It is suggested that only few fine particles (silt) rotate during ageing because the majority of them are not in the strongly loaded force chains, so that they just float within the voids.

Keywords: Microstructures, ageing, K_0 condition, silty sand.

PACS: 89.20.Kk

INTRODUCTION

The macro-mechanical behavior of sand is highly dependent on its particle arrangement and its associated pore spaces, thus its microstructure. Sand ageing is a macroscopic phenomenon which describes the increase in stiffness and strength of a sand over time following disturbance. This occurs under constant effective stress without detectable changes in density.

There is no consensus yet about mechanisms behind sand ageing. In general, there are two main suggested mechanisms, chemical (Mitchell & Solymar, 1984; Sheldon, 2003) and mechanical (Schmertmann, 1991; Bowman & Soga, 2003). This study attempts to enhance our understanding of ageing under mechanical creep behaviour, by investigating microscopic changes that occur during ageing under load. The paper focuses on the initial results for loose silty sand in terms of changes in soil fabric with time.

MATERIAL AND TESTING METHOD

Material

The materials used in this research program were reconstituted in the laboratory by mixing a sand fraction and a fine fraction. Sand particle diameters range from $75\mu\text{m}$ to $300\mu\text{m}$. The fine fraction ($<75\mu\text{m}$, 15% by weight) used in this study is non-plastic silica flour from $32\mu\text{m}$ to $75\mu\text{m}$ (particles smaller than $32\mu\text{m}$ were removed, because they create difficulties for

image analysis). The resultant mean diameter, (d_{50}), maximum and minimum void ratio of e_{max} and e_{min} were $150\mu\text{m}$, 1.026 and 0.645, respectively. Figure 1 shows the particle size distribution of the combined fraction.

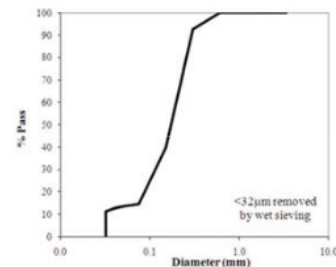


FIGURE 1. Combined particle size distribution.

Sample Preparation for Image Analysis

Specimens were prepared in an impregnation cylinder by moist tamping (Ladd, 1978). While moist tamping does not replicate natural deposition, segregation of fines does not occur as may happen with pluviation and other preparation methods. A low viscosity and shrinkage epoxy curing agent, EPO-THIN, by Buehler Inc. was impregnated into the specimen.

An apparatus to preserve the soil fabric using epoxy resin adapted from Masad (1998) was used with a modification to enable the fitting to be used

2

Powders and Grains 2013

AIP Conf. Proc. 1542, 293-296 (2013); doi: 10.1063/1.4811925

© 2013 AIP Publishing LLC 978-0-7354-1166-1/\$30.00

$$R = \sqrt{\left\{ \sum_{i=1}^N [l_i \sin(2\alpha)] \right\}^2 + \left\{ \sum_{i=1}^N [l_i \cos(2\alpha)] \right\}^2} \quad (1)$$

$$r = \frac{R}{\sum_{i=1}^N l_i} \quad (2)$$

many times. The soil sample, prepared to a relative density of 40%, was loaded to 30kPa under zero lateral strain (K_0 condition). Samples were left under load for periods of one hour and one week, respectively. Muszynski (2000) found significant changes in pore size distribution of silt soil that was left in secondary compression for one hour and for five days, thus similar ageing times were used in this study. The epoxy resin was then injected into the base pedestal of the impregnation chamber under a low pressure. It is possible that injection could cause some disturbance to the finer grains. Nevertheless it can be assumed that disturbances are the same between different samples.

Once the epoxy impregnated specimen was fully cured (about two weeks), it was removed from the impregnation chamber. The sample was then cut, sectioned and polished with successively finer abrasive discs and finally alumina powder.

Capturing Image and Image Processing

Images were taken by high resolution field emission Scanning Electron Microscope (SEM). A back scattered detector (BSD) was used to obtain good quality images (Llyod, 1987). Captured images were then processed and analyzed using image analysis software *ImageJ* and *Image Pro Plus 7.0*. Enhancement of the image involved contrast expansion, correction for noise and thresholding/segmentation. The resulting image the then displayed as a binary image using black and white colours to distinguish foreground and background regions.

Microstructure Measurements

In this study two measures were used to quantify the microstructure changes i.e. particle orientation and distribution of spatial distance between particles.

Particle orientation is usually defined by the angle of the apparent long axis and may be presented visually using a rose diagram. Measurement of the angles was done based on long axis orientation using the *angle* option within *Image Pro Plus* software. Due to a relatively large number of fine particles, in order to avoid bias related to particle size, a weighted value based on area for the orientation of particles is used here. Particle orientation distribution can be analyzed by circular statistics (Fisher, 1993). The properties of

particle orientation distribution can be obtained by the resultant vector length (R), mean resultant length (r), and mean angle (α_m)

$$\alpha_m = \frac{1}{2} \tan^{-1} \left(\frac{\sum_{i=1}^N [l_i \sin(2\alpha_i)]}{\sum_{i=1}^N [l_i \cos(2\alpha_i)]} \right) \quad (3)$$

Where l_i is the length of long axes of the particle, N is the number of measurements, α is the angle between the unit vector and the true direction and r is a measure of the concentration. The value of r ranges from zero to one. When r equals to one, all particles are oriented in the same direction.

Bowman (2002) thought that interlocking of particles may cause soils to age. Interlocking particles are related to particle edges, so that a mean free path method was used in this study to measure the distribution of spatial distance between particles. For this method, a series of scanning lines are drawn which pass through both solid particles and voids (Figure 2b), and the lengths are measured (Kuo, 1998; Masad and Muhunthan, 2000). The directions of the scanning lines used here were vertical and horizontal (Figure 2), commensurate with principal vertical and axisymmetric radial stresses.

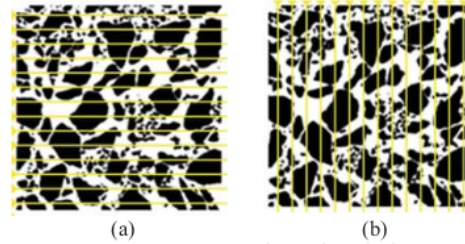


FIGURE 2. Mean free path method

Bowman (2002) suggested the use of variance and kurtosis as statistical measures to assess particle interlock. For an interlocked structure to have the same average density as an unlocked one there must be areas where particles are more clustered and more loosely packed, compared to the unlocked structure. Variance (s^2) is defined as

$$s^2 = \frac{\sum (x - x_m)^2}{n} \quad (4)$$

Where s is standard deviation, x is the log void distance along a scan line, x_m is the mean log void distance and n is the number of samples. Kurtosis is a measure of peakedness of the curve compared to a truly normal curve. In this study it is a measure of

relative number of closely packed particles and large void gaps. It is formulated as below:

$$\beta = \left[\frac{n(n+1)}{(n-1)(n-2)(n-3)} \sum \left(\frac{x - x_m}{s} \right)^4 \right] - \frac{3(n-1)^2}{(n-2)(n-3)} \quad (5)$$

RESULTS

Particle Orientation

Over 5000 particles from 20 images per test were measured for the distribution of particle orientation. Figure 3 shows the mass weighted distribution of particle orientation for all particles. Figure 3a represents rose diagram for one hour ageing time. This provided a 'baseline' of initial fabric against which other tests (one week ageing time in this study), could then be compared. The results indicate that the distribution of particle orientations prepared by moist tamping are fairly random with a slight bias towards a vertical orientation, as found by previous researchers (Jang & Frost, 1998). From the Fisher analysis, Table 1, the mean direction for all particles is 15.5° and mean resultant length r is 0.02844 (near isotropic).

TABLE 1. Particle orientation

Particle	Ageing time	R	r	α_m (°)
All	1 hour	81598	0.02844	15.5
	1 week	138660	0.04847	-34.7
Silt only	1 hour	10128	0.01500	14.3
	1 week	23047	0.03300	25.2
Sand only	1 hour	82087	0.03717	18.1
	1 week	117135	0.05448	94.6

Figure 3b shows the result of the same loading which was applied for one week. This test is compared to the 'baseline' test of one hour (Figure 3a). The rose diagram shows little overall change in the number of particles oriented at various degrees. The mean direction changes to -34.7° compared to 15.5° in the baseline test. This does not suggest much microstructural change considering the bidirectional data of the rose diagram, however, the r value is slightly higher.

It is interesting to then split the data into approximately silt and sand sized particles, as in Table 1. As seen in Figure 4, we see that the orientation of silt-sized particles (with an area less than that of a circle with diameter 75µm) is near isotropic for one hour and one week and little change in mean orientation (14.3° and 25.2° respectively, with low r).

Figure 5 shows only sand-sized particles. We see here that the mean orientation changes from 18.1° to 94.6°, while the dispersion r increases. Hence the majority of particle rotation occurs in the larger group. This may suggest that forces chains mainly consist of larger particles (sand) while fine particles mostly float in the voids between.

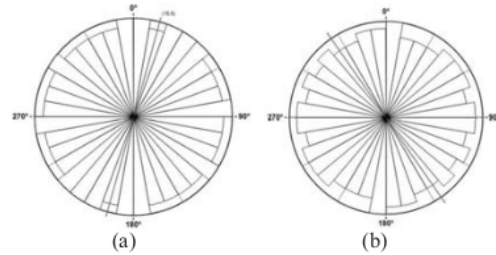


FIGURE 3. Overall rose diagram for 1 hour (a) and 1 week of ageing (b)

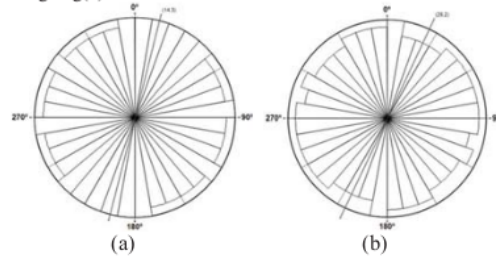


FIGURE 4. Rose diagram of silt-sized particles for 1 hour and 1 week of ageing

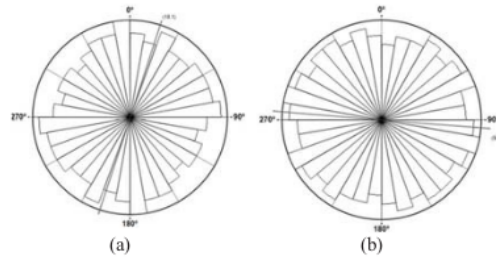


FIGURE 5. Rose diagram of sand-sized particles for 1 hour and 1 week of ageing

Spatial distribution

Figure 6 shows that a typical distribution of particle spacing on a histogram gives a highly right-skewed distribution. In order to be meaningful, this type of distribution should be transformed to approach

normality (Chatfield, 1983). A fitting distribution analysis gives a log normal distribution as the best fit. Thus all data and statistical analysis were performed on log form.

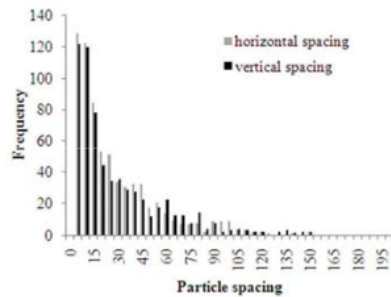


FIGURE 6. Distribution of particle spacing from a typical section

The average spatial distribution results between one hour ageing and one week ageing are shown in Table 2. Generally, the mean log horizontal and vertical spacing are almost the same, indicating an 'isotropic' structure. This is due to the nature of moist tamped samples. Over time there is a slight reduction in mean log spacing both in the horizontal and vertical direction between particles indicating that loading causes a slight decrease in overall global density or void ratio. There is however, very little difference in any of the measures (variance or kurtosis) over time in either horizontal or vertical direction. This may suggest that either that particle clustering is not taking place or that any such change is being masked by the presence of the free-floating fine particles. Further investigation with these small particles being removed by image analysis is on-going to assess the influence of the fines.

TABLE 2. Spatial distribution results

Ageing time	Mean log spacing		Mean Variance s		Mean Kurtosis β	
	H	V	H	V	H	V
1 hour	1.17	1.16	0.21	0.25	-0.93	-0.93
1 week	1.14	1.14	0.24	0.25	-0.92	-0.92

H=Horizontal; V=Vertical

CONCLUSION

This study is attempting to enhance understanding of ageing mechanisms for silty sands, which are common in nature. A scanning electron microscope via electron backscattered detector was used to investigate the microscopic changes that occur during ageing. Image analysis combined with statistical

analysis shows that the orientation of sand-sized particles changes subtly under constant loading over time. However that of silt-sized particles does not change appreciably. It is suggested that few silt particles rotate during ageing because many of them are just floating in the voids. Initial results of spatial analysis suggest that there is little change in the void spacing between particles when the entire particle system is considered. Analysis of the spatial distribution of voids excluding the influence of the fines is on-going, as well as examination of specimens aged for longer time periods.

ACKNOWLEDGMENTS

The Authors would like to thanks Directorate of Higher Education, Ministry of Education and Culture of Indonesia who have funded this research.

REFERENCES

- Mitchell, J. K., & Solymar, Z. V., *Journal of Geotechnical Engineering* **110**, 1559-1576 (1984).
- Sheldon, H. A., & Wheeler, J., *Geological Society of America* **31**, 59-62 (2003).
- Schmertmann, J. H., *Journal of Geotechnical Engineering* **117**, 1288-1330 (1991).
- Bowman, E. T., & Soga, K., *Soils and Foundations* **43**, 107-117 (2003).
- Ladd, R., *ASTM Geotechnical Testing Journal* **1**, 16-23 (1978).
- Masad, E., "Permeability simulation of reconstructed anisotropic soil medium", Phd Thesis, Washington State University, 1998.
- Muszynski, M.R., "Void ratio distribution of Normally consolidated coarse-grain magnetic tailings as a function of aging time", M.S. Thesis, Michigan Technological University, 2000.
- Lloyd, G., "Atomic number and chrysallographic contrast images with the SEM: a review of backscattered electron techniques", *Mineralogical Magazine* **51**, 3-19 (1987).
- Fisher, N.I., *Statistical Analysis of Circular Data*, Cambridge University Press, 1993.
- Bowman, E. T. "The Ageing and Creep of Dense Granular Materials", Phd Thesis, University of Cambridge, 2002.
- Kuo, C. Y., Frost, J.D., and Chameau, J.-L.A., *Geotechnique* **48**, 515-525 (1998).
- Chatfield, C., *Statistic for Technology*. London: Chapman and Hall, 1983.
- Masad, E. & Muhunthan, B., *Journal of Geotechnical and Geoenvironmental Engineering* **126**, 199-207 (2000).
- Jang, D.J and Frost D.J., "Sand Structures Differences resulting from Specimen Preparation procedures," ASCE Specialty Conference on Geotechnical Earthquake Engineering and Soil Dynamic, Seattle, 1998, Vol.1., pp. 234-245.

ORIGINALITY REPORT

8%

SIMILARITY INDEX

8%

INTERNET SOURCES

2%

PUBLICATIONS

%

STUDENT PAPERS

PRIMARY SOURCES

1

geo.shef.ac.uk

Internet Source

3%

2

aip.scitation.org

Internet Source

3%

3

toc.proceedings.com

Internet Source

1%

4

connection.ebscohost.com

Internet Source

1%

5

www.f.waseda.jp

Internet Source

1%

Exclude quotes On

Exclude matches < 1%

Exclude bibliography On